The Peroxisome Deficient Arabidopsis Mutant *sse1* Exhibits Impaired Fatty Acid Synthesis[1][w]

Yun Lin[2]*, Joanne E. Cluette-Brown, and Howard M. Goodman

Department of Genetics, Harvard Medical School, Boston, Massachusetts 02115 (Y.L., H.M.G.); and Department of Molecular Biology (Y.L., H.M.G.) and Department of Pathology, Division of Laboratory Medicine (J.E.C.), Massachusetts General Hospital, Boston, Massachusetts 02114

The Arabidopsis *Shrunken Seed 1* (*SSE1*) gene encodes a homolog of the peroxisome biogenesis factor Pex16p, and a loss-of-function mutation in this gene alters seed storage composition. Two lines of evidence support a function for SSE1 in peroxisome biogenesis: the peroxisomal localization of a green fluorescent protein-SSE1 fusion protein and the lack of normal peroxisomes in *sse1* mutant embryos. The green fluorescent protein-SSE1 colocalizes with the red fluorescent protein (RFP)-labeled peroxisomal markers RFP-peroxisome targeting signal 1 and peroxisome targeting signal 2-RFP in transgenic Arabidopsis. Each peroxisomal marker exhibits a normal punctate peroxisomal distribution in the wild type but not the *sse1* mutant embryos. Further studies reported here were designed toward understanding carbon metabolism in the *sse1* mutant. A time course study of dissected embryos revealed a dramatic rate decrease in oil accumulation and an increase in starch accumulation. Introduction of starch synthesis mutations into the *sse1* background did not restore oil biosynthesis. This finding demonstrated that reduction in oil content in *sse1* is not caused by increased carbon flow to starch. To identify the blocked steps in the *sse1* oil deposition pathway, developing *sse1* seeds were supplied radiolabeled oil synthesis precursors. The ability of *sse1* to incorporate oleic acid, but not pyruvate or acetate, into triacylglycerol indicated a defect in the fatty acid biosynthetic pathway in this mutant. Taken together, the results point to a possible role for peroxisomes in the net synthesis of fatty acids in addition to their established function in lipid catabolism. Other possible interpretations of the results are discussed.

Vegetable oils are an important source of energy and nutrition in human and animal diets. They are also used in the manufacture of paints, inks, lubricants, and other industrial products. The quality and yield of seed oil are important agronomic traits that have been a continuing focus of plant breeding and biotechnology research. A mechanistic understanding of the oil deposition process should facilitate these crop improvement efforts.

Like many crop plants, Arabidopsis accumulates large amounts of oil products in its seeds. In mature Arabidopsis seeds, oil bodies and protein bodies (protein storage vacuoles) occupy over 90% of the cell volume (Lin et al., 1999). Although a transient starch pool is also present in developing embryos, it is mostly remobilized before the embryos mature (Mansfield and Briarty, 1992).

The deposition of seed oil is influenced by multiple metabolic pathways located in various cellular compartments. Suc from the maternal plant serves as the major carbon source for both oil and carbohydrate products. Hexosephosphate derived from Suc cleavage may enter the starch biosynthesis pathway in plastids or the glycolytic pathways in either the cytosol or plastids (Buchanan et al., 2000). By converting the glycolytic product to acetyl-coenzyme A (CoA), the plastidial pyruvate dehydrogenase directs the glycolytic carbon flux to fatty acids (Ke et al., 2000). The large amount of reducing power necessary for fatty acid synthesis may be supplied jointly by pyruvate metabolism and the oxidative pentose phosphate pathway in plastids, as well as by photosynthesis in chloroplasts (Rawsthorne, 2002; Ruuska et al., 2002). In subsequent steps, the fatty acyl chains leave plastids in the form of CoA esters and are assembled in the endoplasmic reticulum (ER) into triacylglycerols to be deposited into oil bodies (Ohlrogge and Jaworski, 1997). Potentially, events that affect any of these metabolic reactions, the biogenesis of relevant organelles, or the interaction among different cellular compartments could all influence oil deposition.

In the reverse of the deposition process, oil is converted to carbohydrates in postgerminative seedlings to provide the carbon and energy required for the establishment of autotrophic growth. Peroxisomes, especially in the form of glyoxysomes, are responsible for this process. In these organelles, the β-oxidation reactions break down acyl-CoA chains to acetyl-CoA, and the glyoxylate cycle reactions convert acetyl-CoA into tricarboxylic acid cycle molecules (Gerhardt, 1992; Eastmond and Graham, 2001). Similar processes occur

[1] This work was supported by the Department of Molecular Biology, Massachusetts General Hospital (grant to H.M.G.).

[2] Present address: Department of Crop Sciences, University of Illinois, Urbana, IL 61801.

* Corresponding author; e-mail yunlin@uiuc.edu; fax 217–244–1707.

[w] The online version of this article contains Web-only data.

Article, publication date, and citation information can be found at www.plantphysiol.org/cgi/doi/10.1104/pp.103.036772.

in senescing tissues to convert lipids into carbohydrates (Poirier et al., 1999; Arai et al., 2002). Although unexpected from the role of peroxisomes/glyoxysomes in fatty acid catabolism, β-oxidation activity can be detected in developing Arabidopsis seeds where net fatty acid synthesis occurs (Arai et al., 2002). More intriguingly, a loss-of-function mutation in the Arabidopsis β-oxidation enzyme 3-ketoacyl-CoA thiolase causes reduced seed oil content (Germain et al., 2001). These observations raise the question as to whether peroxisomal β-oxidation contributes to lipid synthesis, in addition to its obvious function in the degradation process.

Additional evidence indicates that the role of fatty acid β-oxidation is not limited to oil mobilization and senescence. In Arabidopsis, pleiotropic developmental defects are observed after dramatic reduction of fatty acid β-oxidation. Blocking several steps of peroxisomal β-oxidation simultaneously by a mutation in the gene encoding the multifunctional protein AIM1 causes twisted leaves, abnormal inflorescence meristems, and a severe reduction of fertility (Richmond and Bleecker, 1999). Similar phenotypes are found in the *ped1ped3* double mutant, where acyl-CoA import and its subsequent cleavage in peroxisomes are both impaired (Hayashi et al., 2002). Moreover, combination of loss-of-function mutations in the peroxisomal medium- and short-chain acyl-CoA oxidase genes leads to early embryo lethality (Rylott et al., 2003). These phenomena suggest that peroxisomal β-oxidation is essential for normal tissue and organ growth throughout the plant life cycle, but the underlying molecular basis remains elusive.

We have previously reported on an Arabidopsis *sse1* mutant, in which oil and protein body contents are reduced, and instead starch accumulates (Lin et al., 1999). The *SSE1* gene encodes a Pex16p homolog. In the yeast *Yarrowia lypolitica*, the *Yl*Pex16p is required for both peroxisome biogenesis (Eitzen et al., 1997) and mycelial phase specific cell surface protein delivery (Titorenko et al., 1997). The accumulation of small vesicles in the *sse1* mutant led to our speculation that SSE1 is involved in storage organelle biogenesis, possibly through affecting protein or membrane trafficking, as does its yeast homolog. In this manuscript a green fluorescent protein (GFP)-SSE1 fusion protein expressed in transgenic Arabidopsis is shown to be localized to peroxisomes. We also show that the *sse1* mutant embryos lack normal peroxisomes. Thus, a participation in peroxisome biogenesis is at least one of the direct functions of the *SSE1* gene. Further studies detailed in this report reveal substantial reduction of fatty acid synthetic rates in *sse1*. Our results, along with other observations in plants, raise the possibility that loss of peroxisomal functions causes fatty acid and oil deficiency in *sse1*. Given the complexity of the oil deposition process, possible impacts of other cellular and metabolic changes in *sse1* on fatty acid synthesis are also discussed. Further investigation of the metabolic/regulatory roles of peroxisomes and the molecular functions of SSE1 should provide more insight into the altered storage process in the *sse1* mutant.

RESULTS

SSE1 Is Peroxisome-Localized and Overexpression of a GFP-SSE1 Fusion Protein Changes Peroxisome Distribution

The SSE1 coding region was fused in-frame to the C terminus of GFP and placed under the control of cauliflower mosaic virus (CaMV) 35S promoter. Agrobacteria carrying this construct were used to infiltrate the flowers of *sse1*/+ heterozygous plants. Fourteen sustainable transgenic lines were generated. Of these, seven were *sse1*/+ heterozygous and seven were *sse1*/*sse1* homozygous lines as indicated by PCR (Lin et al., 1999). Although these homozygous lines have reduced fertility compared to the wild-type plants, the GFP-SSE1 fusion protein complements both the shrunken seed and the lethal phenotypes (Fig. 1A) of the *sse1* mutant and is therefore functional. Two complemented *sse1/sse1* homozygous lines were randomly selected and cotyledons from young seedlings were observed in a confocal microscope. In both cases, organelles containing the GFP-SSE1 fusion protein varied in their sizes. The prominent ones were much bigger than expected for peroxisomes, and their frequencies often did not exceed one per cell (Fig. 1B and data not shown). Similar distribution of GFP-SSE1 was also observed in developing embryos from four randomly selected transgenic lines of either *sse1/sse1* or *sse1*/+ genotypes (Fig. 1B). As revealed in root cells by fluorescence microscopy, the green fluorescent organelles do not match the 4′-6-diamidino-2-phenylindole (DAPI) stained nuclei (Fig. 1B, see electronic version for higher resolution) and are therefore different structures. Unlike the fusion protein, GFP alone was cytosolic (data not shown), as reported previously (Chiu et al., 1996).

Overexpression of plant peroxisomal membrane proteins has been reported to cause peroxisome clustering (Mullen et al., 2001b). Moreover, overexpression of *Yl*Pex16p in the yeast *Y. lipolytica* resulted in fewer enlarged peroxisomes (Eitzen et al., 1997). This result suggested that the GFP-SSE1-containing organelles might be peroxisomal aggregates or enlarged peroxisomes. Most peroxisomal matrix proteins are directed into the organelle through one of two conserved targeting signals (PTS) located either at the C terminus (PTS1) or at the N terminus (PTS2). The C-terminal 10 amino acids of pumpkin (Cucurbita cv Kurokawa Amakuri) malate synthase contain the PTS1 signal and are sufficient to direct β-glucuronidase into peroxisomes in Arabidopsis (Hayashi et al., 1996). We therefore fused the DNA fragment encoding this peptide to the C terminus of red fluorescent protein (RFP-PTS1). We also fused the predicted PTS2 sequence from Arabidopsis 3-ketoacyl-CoA thiolase (Hayashi et al., 1998; Germain et al., 2001; GenBank

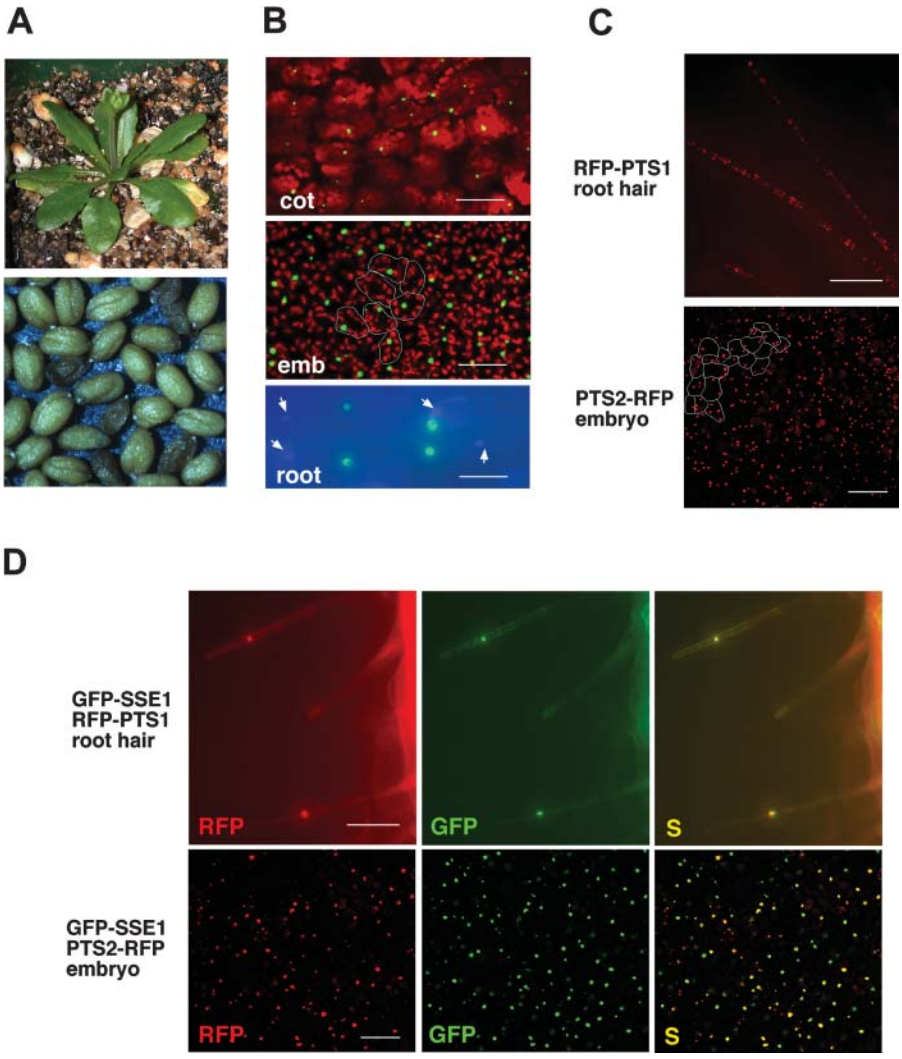

Figure 1. GFP-SSE1 localizes to peroxisomes, and overexpression of GFP-SSE1 changes peroxisome distribution. Cotyledon and embryonic cells were examined by confocal microscopy and root cells were examined by fluorescent microscopy. A, The GFP-SSE1 fusion protein complements the lethal and shrunken seed phenotypes of the *sse1* mutant. The plant and the seeds are from a homozygous *sse1* line expressing the GFP-SSE1 transgene. Segregation of the shrunken seed phenotype is due to segregation of the GFP-SSE1 transgene, i.e. shrunken seeds do not carry the GFP-SSE1 transgene. Complementation was observed in all seven transgenic lines in the *sse1* background. B, GFP-SSE1 containing organelles in young seedlings and developing embryos from GFP-SSE1 transgenic lines. Arrows indicate DAPI stained nuclei. The red color is generated by the autofluorescence of chloroplasts. Estimated borders of several embryonic cells are indicated to show the average cell size. cot, cotyledon cells from a seedling; emb, embryonic cells from a cotyledon stage embryo; root, root cells from a postgerminative seedling. Bar is 80 μm for cotyledon, 30 μm for embryo, and 25 μm for root. C, RFP-PTS1 and PTS2-RFP markers reveal normal peroxisome distributions in wild-type (+/+) or *sse1*/+ plants. The root hair cells are of +/+ and the embryonic cells *sse1*/+ genotypes. Estimated borders of several embryonic cells are indicated to show the average cell size. Bar is 100 μm for root and 50 μm for embryo. D, GFP-SSE1 colocalizes with RFP-PTS1 and PTS2-RFP markers, and overexpression of GFP-SSE1 changes peroxisome distribution. Each peroxisomal marker was introduced into the GFP-SSE1 transgenic line 3 through stable plant transformation. S, The GFP and RFP images are superimposed. Bar is 100 μm for root and 50 μm for embryo.

accession no. AB008854) to the N terminus of RFP (PTS2-RFP). Each of these two RFP-labeled peroxisomal markers was introduced into transgenic plants to visualize peroxisomes.

In young +/+ or *sse1*/+ seedlings, the two RFP markers revealed numerous peroxisomes in each cell. An example of RFP-PTS1 distribution in root hair cells is shown in Figure 1C. In addition, the two RFP markers allowed visualization of peroxisomes in developing Arabidopsis embryos (Fig. 1C for PTS2-RFP, and data not shown), where peroxisomes had not been previously observed. Because transgenic line 3 had GFP-SSE1-labeled organelles in all tissues examined, the two peroxisomal markers were introduced separately into this line to test the peroxisomal localization of SSE1. In contrast to the normal pattern of

peroxisome distribution, many cells of line 3 seedlings contained only one enlarged peroxisome (or peroxisomal aggregate) per cell as revealed by both RFP markers. Figure 1D shows an example of a single RFP-PTS1-labeled peroxisome (or peroxisomal aggregate) in a root hair cell. Similarly, reduction in number and increase in the average size of peroxisomes were also observed in developing embryos of line 3 (compare Fig. 1D and 1C), although the effect in embryo was not as dramatic as in seedling. The distribution of RFP-labeled peroxisomes in line 3 resembled that of GFP-SSE1, and superimposed images of GFP and RFP confirmed that SSE1 colocalizes with each peroxisomal marker (Fig. 1D). Therefore, SSE1 is targeted to peroxisomes, and overexpression of this protein changes peroxisome distribution.

We also used electron microscopy (EM) to examine peroxisomes in cotyledons and true leaves from young seedlings. In contrast to the typical peroxisomes in wild-type plants (Fig. 2A), aggregates of approximately 20 peroxisomes were found in the EM sections from line 3 (Fig. 2, B–D). Frequently, neighboring peroxisomes were fused to one another (Fig. 2, C and D). These aggregates are likely the large green fluorescent organelles observed by fluorescence and confocal microscopy (Fig. 1, B and D). Single peroxisomes corresponding to the relatively smaller green fluorescent structures were also observed by EM (data not shown). In addition, chloroplasts in the transgenic plants appeared to have less organized thylakoid membranes (Fig. 2B). This might be a consequence of the abnormal peroxisomal distribution, as the two organelles are normally closely positioned as they carry out coordinated functions such as photorespiration.

sse1 Embryos Lack Normal Peroxisomes

The RFP-PTS1-labeled peroxisomes could be observed in +/+ or *sse1*/+ embryos by fluorescent microscopy. However, the *sse1* mutant embryos from the same *sse1*/+ lines did not have a detectable RFP signal (Fig. 3A). The fusion protein was possibly degraded in the mutant when it was unable to localize to peroxisomes. The other marker, PTS2-RFP, also demonstrated the lack of normal peroxisomes in *sse1* (Fig. 3B). In contrast to its punctate distribution pattern

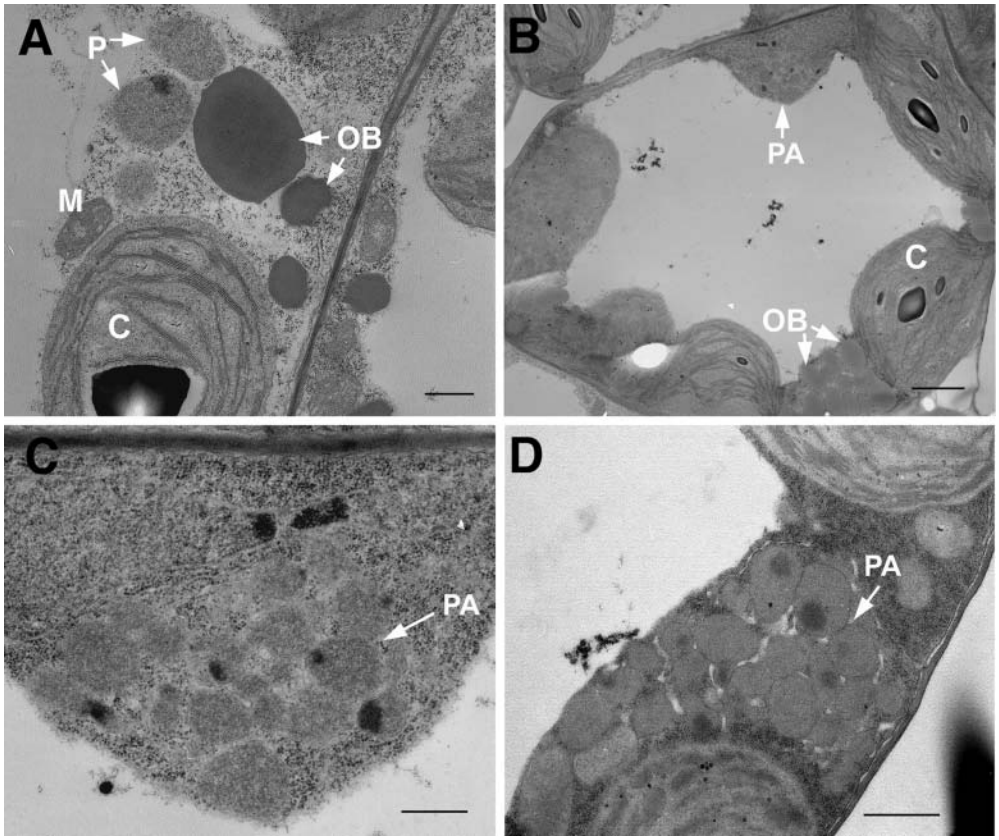

Figure 2. GFP-SSE1 overexpression causes partially fused peroxisomal aggregates. A, Typical peroxisomes in the cotyledon of a wild-type seedling. Bar is 500 nm. B, A cotyledon cell in a seedling from GFP-SSE1 transgenic line 3. A peroxisomal aggregate is present. Bar is 2 μm. C, Enlargement of the peroxisomal aggregate in B. Peroxisomes are fused to each other at some areas. Bar is 500 nm. D, A peroxisomal aggregate in a mesophyll cell from a true leaf of GFP-SSE1 transgenic line 3. Peroxisomes are fused to each other in some areas. Bar is 1 μm. P, peroxisome; PA, peroxisomal aggregate; OB, oil body; C, chloroplast; M, mitochondrion.

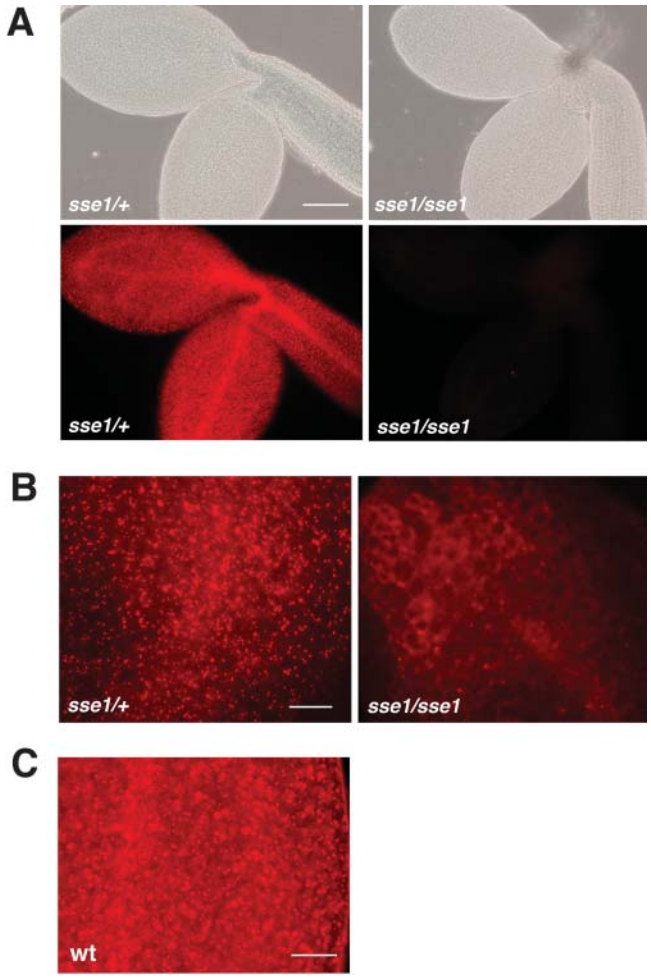

Figure 3. RFP-labeled peroxisomes in wild-type (or *sse1*/+ heterozygous) and *sse1* embryos revealed by fluorescence microscopy. A, Heterozygous (*sse1*/+) and *sse1* mutant (*sse1*/*sse1*) embryos from an RFP-PTS1 transgenic line. Bright field images of the embryos are also shown. Bar is 150 μm. B, Heterozygous (*sse1*/+) and *sse1* mutant (*sse1*/*sse1*) embryos from a PTS2-RFP transgenic line. Bar is 40 μm. C, RFP-PTS1 labeled peroxisomes in mature wild-type embryos. Bar is 40 μm.

in heterozygotes, PTS2-RFP had a diffuse distribution in *sse1*, suggesting that it is located either in the cytosol or in small structures that may be remnants of peroxisomes. The fact that neither the PTS1 nor PTS2 constructs revealed peroxisomes indicates that the *sse1* mutant probably has lost most peroxisomal functions, as have yeast and human *pex16* mutants (Eitzen et al., 1997; Honsho et al., 1998; South and Gould, 1999). Peroxisomes are also present in mature wild-type Arabidopsis embryos. Although the background RFP signal (nonspecific localization of the fusion protein to the protein bodies) became stronger as the embryos matured, the signal from the peroxisomes was more intense and could easily be recognized (Fig. 3C, see electronic version for higher resolution).

If peroxisome biogenesis occurs during embryogenesis, peroxin genes should be expressed in developing seeds. We have shown previously that the expression of the *SSE1* gene in whole siliques increases as the seeds mature (Lin et al., 1999). In order to measure peroxin gene expression from seed tissues exclusively, seeds from 7 days after fertilization (DAF) until full maturation were used for gene expression analysis. The mRNA levels of eight peroxin genes were compared among seeds, flower buds, seedlings, and emerging leaves by use of a semiquantitative reverse transcription-PCR (RT-PCR). These genes were detected in all tissues, and, for most of them, the steady state mRNA levels in mature seeds were at least as high as that in developing seeds (Fig. 4). In addition, all eight genes were strongly expressed in flower buds, indicating that high peroxisome activities might be present in this tissue. By contrast, the mRNA level of *Leafy Cotyledon 1* (*LEC1*), a global regulator of embryogenesis, decreased continuously in seeds after the early cotyledon stage and was barely detectable in seedlings, flower buds, or leaves (Lotan et al., 1998). Another control gene, *Actin 2* (*ACT2*), was constitutively expressed in all tissues and developmental stages tested (An et al., 1996).

sse1 Developing Embryos Exhibit Reduced Rates of Fatty Acid Synthesis

To understand the reduction of oil content in *sse1*, we compared the time courses of oil accumulation in developing wild-type and *sse1* embryos. Because the opposite changes in starch and oil contents in *sse1*

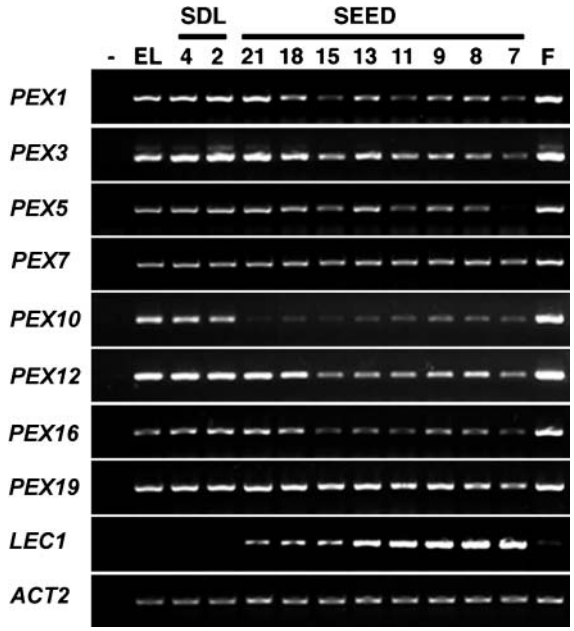

Figure 4. Semiquantitative RT-PCR analyses of gene expression. RNA was isolated from flower buds (F), 7- to 21-DAF seeds (SEED), 2- and 4-d-old seedlings (SDL), and emerging leaves (EL). The same cDNA mixture was used to amplify different fragments through 30 to 40 cycle PCR reactions. PCR without cDNA templates was conducted simultaneously as a negative control (−). The *PEX16* gene is *SSE1*. *LEC1*, *Leafy Cotyledon 1*; *ACT2*, *Actin 2*.

seeds may have a cause and effect relationship (Lin et al., 1999), we analyzed the time course of starch accumulation as well. Embryos of various developmental stages were separated from endosperm and seed coats, and those *sse1* embryos with clear developmental delays were not used (see below and Supplemental Fig. 1S, which can be viewed at www.plantphysiol.org). At 9 DAF, starch levels were still low in both mutant and the wild type, while the *sse1* mutant already had detectably higher amounts of starch (0.08 ± 0.03 μg/embryo in wild type and 0.25 ± 0.11 μg/embryo in *sse1*). During the seed filling period, *sse1* accumulated starch at elevated rates, and the period of net starch degradation started later than in wild type. As a consequence, the starch level in the *sse1* mutant at 22 DAF (mature embryo) was much higher than the peak level in the wild type at 13 to 15 DAF. In contrast to starch, the oil time course had an opposite trend in *sse1*. Severely reduced oil contents and decreased rates of oil accumulation were observed throughout the seed filling period in *sse1* (Fig. 5A). To rule out the possibility that the low rate of oil accumulation in *sse1* was simply a consequence of increased carbon flux into starch, we assessed the effect of abolishing starch synthesis on the production of oil in *sse1*. As shown in Figure 5B, although starch accumulation was prevented by introducing the starch synthesis mutants *adg1* (Lin et al., 1988; Wang et al., 1998) or *pgm1* (Caspar et al., 1985, Periappuram et al., 2000) into the *sse1* background, the levels of oil in the *sse1adg1* or *sse1pgm1* double mutants and the *sse1* single mutant (all in the *C24* and *Col* hybrid background) were indistinguishably low, less than 10% of that in wild type *C24* or *Col*. These results demonstrated that the low rate of oil deposition in *sse1* was not caused by the increased starch synthesis. Indeed, the loss of carbon from the oil pool was more striking than the gain of carbon in the starch pool (Fig. 5, A and B) and, Suc, the major carbon source used for the synthesis of both oil and starch, accumulated in mature *sse1* seeds (Fig. 5C).

In order to determine the location of the block in the *sse1* oil deposition pathway, we fed *sse1* developing embryos radiolabeled oil synthetic precursors and measured their incorporation into oil. The biosynthetic pathways for oil and starch diverge after the synthesis of Glc-6-phosphate (Glc6P). Conversion of Glc6P to Glc-1-phosphate by the plastidial phosphoglucomutase commits the carbon flux to starch. Cytosolic or plastidial glycolysis followed by acetyl-CoA formation in plastids, on the other hand, directs the carbon flux toward fatty acids, which are then used to synthesize oil or other lipids. Because starch synthesis is elevated in *sse1* embryos, the defect in oil deposition should be downstream of Glc6P on the oil branch and possibly causes shifted carbon flux toward starch.

As expected, oil in the *sse1* embryos incorporated small amounts of label from Glc (Fig. 5D), which enters fatty acid biosynthesis upon conversion to Glc6P by hexokinase. Control experiments showed that Glc was taken up and incorporated into starch, cell wall, and proteins (80% ethanol insoluble fraction) in both the wild-type and the *sse1* embryos (Fig. 5E). Pyruvate and acetate, which are converted to the downstream precursor acetyl-CoA by the plastidial pyruvate dehydrogenase and acetyl-CoA synthase, respectively, also failed to support oil synthesis in *sse1* embryos (Fig. 5D). However, both pyruvate and acetate were taken up and metabolized by the *sse1* embryos as efficiently as the wild type (Fig. 5E). In contrast to these results, oleic acid was able to support oil synthesis in *sse1* embryos at rates at least as high as that of the wild-type embryos (Fig. 5D). The capability of *sse1* to synthesize oil from fatty acids but not acetyl-CoA suggests impaired fatty acid synthesis. This is likely to be the direct cause of the reduced oil content in *sse1* seeds.

Tween-Fatty Acid Esters Partially Rescue Early Seedling Arrest of the *sse1* Mutant

It has been shown previously that plants can incorporate fatty acids into their membranes from tween-fatty acid esters (Terzaghi, 1989). To determine whether shortage of fatty acids is also the cause of other developmental defects in *sse1*, we grew *sse1* seedlings on culture medium supplemented with Tween 80 (polyoxyethylene sorbitan esterified to oleic acid). After being dissected from their seed coats, about 40% to 70% of mature *sse1* embryos could develop into small seedlings. In the absence of exogenous fatty acids, the *sse1* mutant seedlings exhibited little root and shoot growth. The shoot appeared to contain one to three leaf-like small structures that failed to expand or turn green (Fig. 6). In the presence of Tween 80, about 10% of *sse1* seedlings produced many small green leaves with a water-soaked and translucent appearance. Elongated roots were sometimes observed in seedlings grown on Tween 80 (data not shown). In the control wild-type seedlings, Tween 80 did not affect seedling growth (Fig. 6). Thus, limited fatty acid synthesis at least partially explains the growth defects of the *sse1* mutant.

sse1 Mutant Seeds Have an Altered Fatty Acid Composition

The fatty acid composition of triacylglycerols was compared between *sse1* and wild-type seeds (Table I). C_{16}, C_{18}, and C_{20} fatty acid chains as percentage of total fatty acids were similar between *sse1* and wild-type seeds. However, *sse1* seeds exhibited approximately two-fold reductions in the saturated fatty acids 18:0 and 20:0 and the polyunsaturated fatty acids 18:2 and 20:2, but modest increases in the monounsaturated fatty acids 18:1 and 20:1 and the polyunsaturated fatty acid 18:3. For unknown reasons, *sse1* contained a much higher proportion than wild-type seeds of the $\omega 7$ series of monounsaturated fatty acids. The saturated fatty acid 18:1 ($\omega 7$) was only 1.1% and 20:1 ($\omega 7$) 1.2% of the total fatty acids in wild-type seeds as compared to

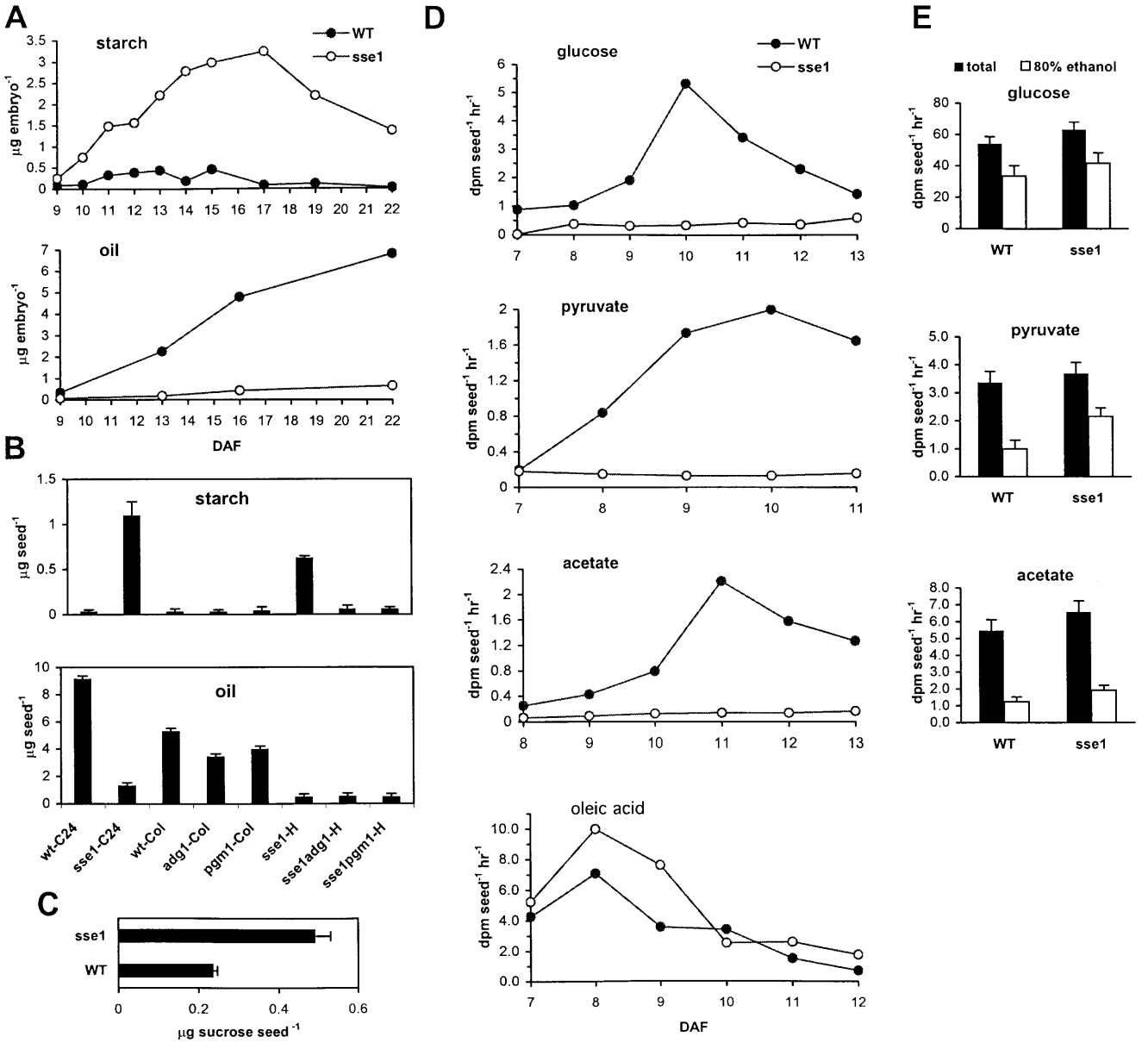

Figure 5. *sse1* embryos exhibit reduced rates of fatty acid synthesis. A, Time course of starch and oil accumulation in wild-type (black circles) and developmentally advanced *sse1* (white circles) embryos dissected from seed coats. The time course is determined from late torpedo and early cotyledon stage (9 DAF) until the mature embryo stage (22 DAF). Developmentally delayed *sse1* embryos were excluded from the experiment. For each time point, 15 to 40 and 10 to 30 embryos were pooled for starch and oil determination, respectively. Each starch extract was measured twice and the error is less than 10% for values greater than or equal to 0.1 μg embryo^{-1} (except *sse1* at 9 DAF where it was 0.25 $\pm$ 0.11 μg embryo^{-1}). Each FAME extract was measured once. B, Starch and oil contents in the *sse1adg1* and *sse1pgm1* double mutant seeds. The original *sse1* single mutant is in the *C24* background (*sse1-C24*). The *adg1* and *pgm1* single mutants are in the *Col* background (*adg1-Col* and *pgm1-Col*). The *sse1adg1* and *sse1pgm1* double mutants are in the *C24* and *Col* hybrid background (*sse1adg1*-H and *sse1pgm1*-H). Results from wild-type *C24* (wt-*C24*) and *Col* (wt-*Col*) seeds, as well as *sse1* single mutant seeds in the *C24* and *Col* hybrid background (*sse1*-H), are shown as controls. Bars are SES. C, Suc contents in mature wild-type *C24* (wt-*C24*) and *sse1* seeds. Bars are SES. D, Incorporation of ^{14}C-labeled precursors into triacylglycerol in developing *sse1* and wild-type *C24* seeds. Single representative experiments of two to three replicates are shown. Among different sets of experiments, seeds of the same developmental stage may differ in actual age of up to 1 DAF, due to seasonal or other variations. E, Oil synthesis precursors taken up and metabolized by the *sse1* mutant embryos. Embryos of 11 to 12 DAF were fed [U-^{14}C]Glc, [2-^{14}C]pyruvate, or [1-^{14}C]acetate as in D and washed with water before measurement of the total amount of label remaining in the embryo (total; black bars) and the amount incorporated into the 80% ethanol insoluble fraction (80% ethanol; white bars).

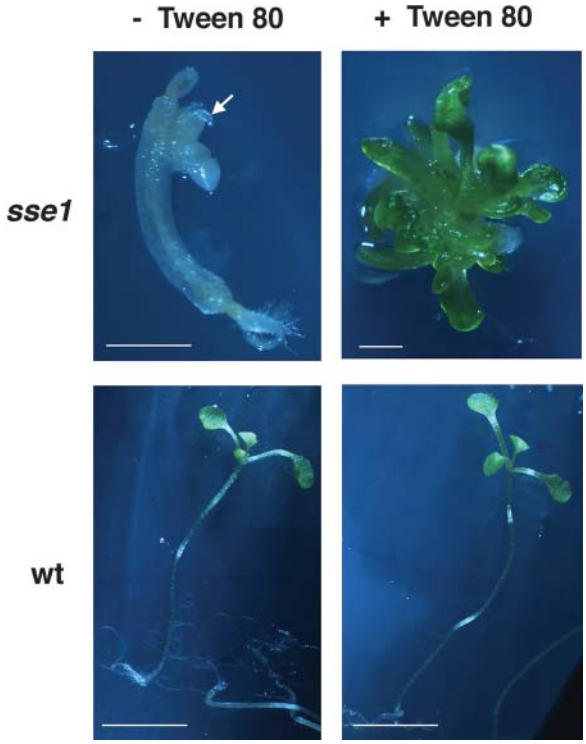

Figure 6. Tween 80 rescue of *sse1* seedling growth. Arrows indicate shoot-like tissues in *sse1* seedlings in the absence of Tween 80. In the presence of Tween 80, about 10% of the *sse1* seedlings produce small and green translucent leaves. The *sse1* seedling on Tween 80 is 4 weeks old, and all other seedlings are 3 weeks old. Bars are 4.0 mm for wild-type and 0.46 mm for *sse1* seedlings.

6.5% and 8.8%, respectively, in *sse1* seeds. Even though the total amount of fatty acids (μg seed^{-1}) was reduced approximately seven-fold in *sse1* seeds (Fig. 5B), the levels of 18:1 (ω7) and 20:1 (ω7; μg seed^{-1}) in *sse1* seeds were close to that in the wild-type seeds (approximately 0.1 μg seed^{-1} each).

The Embryonic Defects of *sse1* Mutant

The *sse1* and wild-type embryos of various developmental stages were compared. The *sse1* embryos exhibited an impaired greening process. At late torpedo and early cotyledon stages (at 8 DAF; Fig. 7A), the wild-type embryos turned green, while *sse1* embryos stayed yellow-white. In a population segregating for approximately 90% of *sse1/sse1* and 10% of *sse1/+* genotypes (Lin et al., 1999), the few green *sse1/+* embryos could be distinguished from the *sse1/sse1* majority (Fig. 7A). In addition, *sse1* embryos exhibited various degrees of developmental delay during early morphogenesis. By 8 DAF, most wild-type embryos entered late torpedo or early cotyledon stage, whereas about 50% of 8-DAF *sse1* embryos were still at the early torpedo or heart stage (Fig. 7A). Throughout the seed-filling period, the developmentally advanced *sse1* embryos appeared to be smaller than the wild type (Fig. 7B), and this size difference persisted into the mature seed stage (Fig. 7C). Comparison in a transmission light microscope revealed smaller cotyledon areas and thinner hypocotyls in 11-DAF *sse1* (Fig. 7B). Both the reduction in storage products and the growth deficiency may restrict *sse1* embryo expansion.

DISCUSSION

SSE1 Is Required for Peroxisome Biogenesis in Arabidopsis

We showed previously that *SSE1* encodes a Pex16p homolog in Arabidopsis and is able to complement *Y. lipolytica pex16* mutants (Lin et al., 1999). Using a GFP-SSE1 fusion protein that complements *sse1* mutant phenotypes at the seed and vegetative developmental stages, together with two RFP-labeled peroxisomal markers, we show here that SSE1 localizes to peroxisomes. Using the RFP markers, we further illustrate the lack of normal peroxisomes in the *sse1* mutant and therefore confirm that the SSE1 protein functions as a peroxin in Arabidopsis. Consistent with our results, a transiently expressed myc-epitope-tagged SSE1 protein (*myc-At*Pex16p) was recently localized to peroxisomes in tobacco Bright-Yellow 2 and Arabidopsis suspension culture cells. In addition, localization of *myc-At*Pex16p to an ER-like preperoxisomal compartment was also observed in these systems, indicating that SSE1/*At*Pex16p may be involved in an ER-dependent step of peroxisome biogenesis (Karnik, 2003).

The CaMV 35S promoter-directed overexpression of the GFP-SSE1 fusion protein results in one or a few aggregates of partially fused peroxisomes per cell. Because as many as 20 aggregated peroxisomes were observed in a single EM section, the estimated number of peroxisomes in a spherical aggregate may be over 60 (spherical volume calculated from cross-sectional area). This explains the dramatic alteration of peroxisome

Table I. *Fatty acid composition of wild-type C24 and sse1 mutant seeds*

Fatty Acid	Wild Type *C24*[a]	*sse1*[a]
	%	
16:0	10.0 ± 0.3	9.0 ± 0.6
18:0	6.6 ± 0.3	3.4 ± 0.3
18:1 (total)	16.9 ± 0.2	25.2 ± 0.9
18:1 (ω9)	15.8 ± 0.2	18.7 ± 1.1
18:1 (ω7)	1.1 ± 0.1	6.5 ± 0.9
18:2	21.5 ± 0.5	11.6 ± 0.6
18:3	19.1 ± 0.3	23.1 ± 0.9
20:0	4.0 ± 0.2	1.9 ± 0.3
20:1 (total)	17.6 ± 0.5	21.9 ± 1.3
20:1 (ω9)	16.4 ± 0.5	13.1 ± 1.0
20:1 (ω7)	1.2 ± 0.1	8.8 ± 0.7
20:2	1.8 ± 0.1	1.0 ± 0.1
20:3	0.5 ± 0.1	0.5 ± 0.2
22:0	0.4 ± 0.1	0.5 ± 0.1
22:1	1.8 ± 0.1	2.0 ± 0.1

[a]Values are in percentage ± SE.

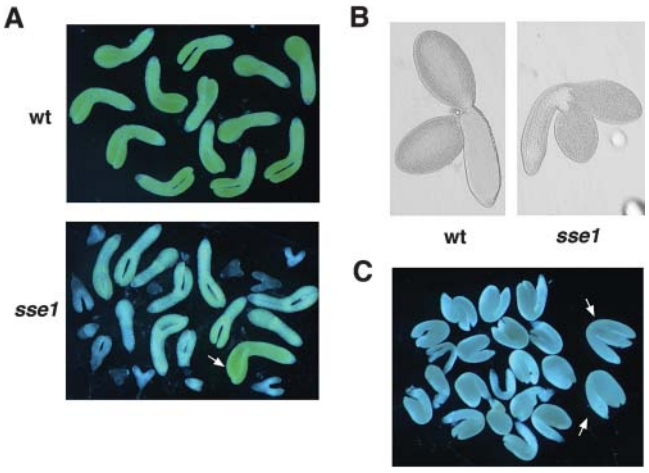

Figure 7. The developmental defects of the *sse1* mutant. A, Embryos from an 8-DAF silique of a wild-type *C24* and a heterozygous *sse1/+* plant. Arrow indicates a green heterozygote *sse1/+* embryo in the segregating population. B, The 11-DAF wild-type *C24* and *sse1* embryos as seen in the light microscope. C, Mature embryos from a dry silique from a heterozygous *sse1/+* plant. Seeds were soaked in water for a few hours to reduce the shrunken appearance before embryos were dissected from the seed coats. Two heterozygote embryos in the population are indicated with arrows.

distribution observed in GFP-SSE1 overexpressing plants.

It was reported previously that overexpression of a peroxisomal membrane protein ascorbate peroxidase (Mullen et al., 2001b) in tobacco Bright-Yellow 2 cells caused peroxisomal clustering. Moreover, when a membrane-targeting peptide from ascorbate peroxidase was fused to GFP, overexpression of the fusion protein caused homotypic and heterotypic aggregates of peroxisomes, mitochondria, and/or plastids (Lisenbee et al., 2003). These results were interpreted as oligomerization of the overexpressed cytosol-facing membrane proteins causing organelle aggregation. A similar cause could be responsible for the peroxisomal aggregates in our GFP-SSE1 transgenic plants, and therefore the altered organelle distribution may be unrelated to the specific function of SSE1. Interestingly, overexpression of the SSE1/*At*Pex16p homolog *Yl*Pex16p results in fewer enlarged peroxisomes in the yeast *Y. lypolitica* (Eitzen et al., 1997), and this phenomenon was attributed to a different mechanism. A multistep peroxisomal assembly pathway that involves several vesicular intermediates has been proposed in *Y. lipolytica* (Titorenko et al., 2000). *Yl*Pex16p is believed to inhibit the division and proliferation of early intermediates. Overexpression of *Yl*Pex16p causes constitutive inhibition of peroxisome division and therefore a reduction in number but increase in size of peroxisomes (Guo et al., 2003). Because SSE1/*At*Pex16p complements the *Y. lypolitica pex16* mutant (Lin et al., 1999), our results do not rule out the possibility that the altered peroxisome distribution in GFP-SSE1 transgenic plants reflects a similar role of SSE1/*At*Pex16p in peroxisome biogenesis. In this case, those partially fused (or connected) peroxisomes would be the outcomes of incomplete peroxisome divisions.

The yeast *pex16* mutants cannot assemble normal peroxisomes but instead accumulate small peroxisomal remnants (20–50 nm in diameter versus 200–500 nm normal size) (Eitzen et al., 1997). Many peroxisomal proteins are completely or partially mislocalized and peroxisomal metabolism is impaired. Because of deficient peroxisomal fatty acid β-oxidation, the yeast *pex16* mutants fail to grow on oleic acid as the sole carbon source (Eitzen et al., 1997). Perhaps even more severe than the yeast mutants, the human *pex16* patients are defective in peroxisomal membrane assembly and lack any detectable peroxisomal remnants (South and Gould, 1999; Honsho et al., 1998). In order to visualize peroxisomes easily in Arabidopsis (especially in the embryos), we fused RFP to PTS1 and PTS2, the predominant peroxisomal localization signals among all matrix proteins. These RFP markers illustrated that the *sse1* mutant lacks normal peroxisomes. The diffuse distribution of PTS2-RFP observed in *sse1* (Fig. 3B) indicates that the marker is localized either in very small aberrant structures or ectopically in the cytosol. On the other hand, the absence of detectable RFP-PTS1 in *sse1* suggests that the peroxisomal remnants (if there are any) are missing at least a subset of matrix proteins. Thus, similar to the yeast and human *pex16* mutants, *sse1* cannot assemble normal peroxisomes and is likely to have impaired peroxisomal metabolism including fatty acid β-oxidation.

The sse1 Mutant Exhibits a Substantial Reduction in Oil Content and a Reduced Rate of Fatty Acid Synthesis

In *sse1* seeds, oil is reduced to approximately 10% to 16% of the wild-type level; starch is increased from a negligible amount to approximately 1.1 to 1.5 μg/seed (Fig. 5, A and B); and storage protein content is approximately 30% to 60% of the wild-type level. The decrease of storage protein content is less severe than that of the protein bodies (Y. Lin and H.M. Goodman, unpublished data). We suspect that some of the storage proteins are in vesicles or other compartments and that defects in protein body biogenesis, rather than protein synthesis, is likely to be the primary cause of protein content reduction. The impact of the *sse1* mutation on oil is the most dramatic among the three storage pools. Analysis of the double mutants *sse1adg1* and *sse1pgm1* (Fig. 5B) shows that the reduction of oil in *sse1* is not caused by increased carbon flow to starch. To locate the blocked step on the oil deposition pathway, we fed *sse1*-developing seeds radiolabeled oil precursors. Reflecting the slower oil accumulation process in *sse1* (Fig. 5A), radiolabeled Glc, pyruvate, and acetate are incorporated into oil at dramatically reduced rates while being taken up and metabolized into starch, cell wall, or protein at normal levels (Fig. 5,

D and E). Although different internal metabolite pool sizes may cause different dilutions of isotopes in *sse1* and the wild-type seeds, the rates of isotope incorporation in *sse1* were reduced so substantially that they likely indicate a real reduction of synthetic rates, at least qualitatively. Because pyruvate and acetate are converted to plastidial acetyl-CoA through different routes, the defective process in *sse1* is likely to be downstream of acetyl-CoA. In contrast, oleic acid (18:1), a major fatty acid synthesized in the plastids and the predominant source of acyl-CoA chains for oil synthesis in the ER in Arabidopsis, enters the oil pool at a rate similar to that of the wild type (if not higher). Thus, steps downstream of fatty acids are likely to be intact in *sse1*.

The radiolabeled metabolites were incorporated at the maximum rates at or before 11 DAF in isolated wild-type seeds (Fig. 5D), whereas the rate of oil accumulation remained high after 11 DAF in vivo (Fig. 5A). There are at least two possible reasons for the observed differences. First, the feeding experiments were designed to measure steps downstream of Glc6P, although upstream steps, such as Suc uptake and conversion, also contribute to the kinetics of oil synthesis. Ruuska et al. (2002) have shown that the expression of Suc synthase increases from 8 DAF to at least 12 DAF. Second, the isolated seeds may have different physiologies and therefore a different oil synthesis time course compared to the normal growing seeds.

Other developmental defects observed in *sse1*, such as its impaired greening process and early embryo/seedling developmental defects, might also be partly due to fatty acid deficiency. Both thylakoid membrane assembly and organogenesis rely on high rates of fatty acid synthesis and might be restricted by an inadequate supply. In support of this view, tween-fatty acid esters can partially rescue *sse1* developmental defects (Fig. 6). The reason why Tween 80 rescued only a subset of *sse1* mutant seedlings is not clear yet. Nonetheless, given the quantitative nature of *sse1* developmental abnormalities (variation in the onset and the degree of defects), it is possible that the mutant seedlings responding to Tween 80 suffered the least developmental impairment during embryonic and early seedling growth.

The Possible Causes of Fatty Acid Synthesis Defects in *sse1*

Defects in ER Functions

Karnik (2003) reported that SSE1/*At*Pex16p is localized to an ER-like preperoxisomal compartment before targeting to peroxisomes. Thus, SSE1 is sorted through the ER to peroxisomes. One may speculate that if the ER functions are disturbed in the *sse1* mutant because protein and membrane sorting to downstream compartments is impaired, this may cause perturbation of lipid metabolism in the ER. Possibly, the abnormal lipid metabolism in the ER inhibits fatty acid synthesis in the plastids. The drawback of this hypothesis is the difficulty in explaining the specificity of the defect. Since *sse1* is able to synthesize oil from fatty acids at normal rates (Fig. 5D), perturbation of the ER must be specific enough to affect only those metabolic enzymes that are not in the Kennedy pathway (Kennedy, 1961). This hypothesis is formally possible, but it is at least equally possible that the fatty acid deficiency in *sse1* is directly linked to peroxisomes, which are known to be involved in lipid metabolism.

Defects in Peroxisome Metabolism

Peroxisomes are known to compartmentalize fatty acid β-oxidation, and their function in lipid catabolism is well-recognized (Gerhardt, 1992). Interestingly, β-oxidation activities are also present in normal developing Arabidopsis seeds (Arai et al., 2002), indicating that β-oxidation might be required even for the net synthesis of fatty acids. Moreover, in transgenic *Brassica napus* overexpressing the lauryl-acyl carrier protein (Eccleston and Ohlrogge, 1998) and in the Arabidopsis diacylglycerol acyltransferase mutant (Poirier et al., 1999), production of fatty acids exceeds the demand (or capacity) of oil synthesis, causing excess carbon chains to enter the β-oxidation pathway. These observations suggest that mechanisms exist to constantly adjust the synthesis and degradation processes. Because fatty acids and their derivatives have important structural and regulatory roles, such a balance is probably critical for the maintenance of normal metabolic and cellular functions. In *sse1*, perhaps fatty acid synthesis slows down as the consequence of impaired peroxisomal β-oxidation. We speculate that negative feedback by fatty acid-derived molecules (Ohlrogge and Jaworski, 1997) might contribute to achieving an appropriate balance between synthesis and degradation.

The role of β-oxidation in oil synthesis is supported by the modestly decreased seed oil content of the Arabidopsis 3-ketoacyl-CoA thiolase mutant *kat2* (Germain et al., 2001). Further reduction of oil content in *kat2* seeds is likely to be prevented by the other thiolase genes *KAT5* (At5g48880) and *KAT1* (At1g04710). In the current GenBank release, the frequencies of expressed sequence tag clones from developing seeds or green siliques for *KAT2* (20), *KAT5* (8), and *KAT1* (3) indicate that *KAT5* and *KAT1* together may contribute 30% of the thiolase activity in seeds. Consistent with the observations in plants, disrupted gene expression of fatty acid β-oxidation enzymes in *Caenorhabditis elegans* reduces body fat (Ashrafi et al., 2003).

The essential role of fatty acid β-oxidation during plant development has been demonstrated by independent lines of evidence. In the Arabidopsis acyl-CoA oxidase 3 and 4 (*acx3acx4*) double mutant, abolishing β-oxidation results in early embryonic lethality (Rylott

et al., 2003). In the peroxisome deficient 1 and 3 (*ped1ped3*) double mutant and the abnormal inflorescent meristem (*aim1*) single mutant of Arabidopsis, severe attenuation of the β-oxidation pathway causes seriously perturbed reproductive growth and abnormal leaf development (Hayashi et al., 2002; Richmond and Bleecker, 1999). The accumulation or depletion of regulatory molecules has been proposed previously as possible reasons for these pleiotropic developmental defects (Richmond and Bleecker, 1999).

Besides fatty acid β-oxidation, peroxisomes compartmentalize other reactions. In mammals, these organelles are known to accommodate diverse lipid metabolic functions such as the biosynthesis of etherphospholipids (plasmalogen), docosahexaenoic acid, cholesterols, bile acids, and the α-oxidation of phytanic acid (Wanders, 1999; Kovacs et al., 2002). In plants, they are the sites of the glycolate pathway, glyoxylate cycle, and ureide pathway (Olsen et al., 1998). The large number of predicted peroxisomal resident proteins in the Arabidopsis genome (Kamada et al., 2003) indicates that the full spectrum of metabolic reactions is yet to be uncovered. It is therefore unclear yet whether plant peroxisomes participate in lipid metabolism as extensively as mammalian peroxisomes. The biosynthesis of the lipid-signaling molecule jasmonic acid is at least one known example (Weber, 2002). Given the complexity of peroxisomal metabolisms, there remains the possibility that an impaired chemical process other than β-oxidation in *sse1* affects fatty acid synthesis through metabolic interactions or signaling events.

Other Developmental Defects

The *sse1* mutant embryos show different degrees of developmental delay or arrest (Fig. 7). Similar but more severe developmental arrest also occurs in the Arabidopsis peroxisome biogenesis mutants *pex2* (Hu et al., 2002) and *pex10* (Sparkes et al., 2003), which are both embryo lethal. The lethality of plant peroxisomal biogenesis mutants indicates the general importance of these small organelles for survival. In this sense, plant peroxisome defects might be similar to the manifestation of the Zellweger disease in humans (Wanders, 1999), although the exact causes of the lethality may not be identical. It seems unlikely, however, that the fatty acid deficiency in *sse1* is secondary to the general developmental defects. Among developmentally advanced *sse1* embryos, oil content is reduced to 10% of that in the wild type, a reduction much more severe than either the developmental delay or the embryo size reduction (Fig. 5A and Supplemental Fig. S1). The dramatically elevated starch synthesis is not the consequence of a general growth arrest, but likely the consequence of a specific reduction of oil content.

One developmental factor that may attenuate fatty acid synthesis in *sse1* is the impaired chloroplast function. The *sse1* mutant exhibits both fatty acid and chloroplast defects, and it is not clear whether one is the cause of the other. The fact that Tween 80 allows greening suggests that the lack of greening is largely a consequence of fatty acid deficiency. However, we do not rule out the possibility that, if the biogenesis of the two organelles is coordinated, disordered peroxisome assembly itself prevents optimum chloroplast development in *sse1.*

In developing green seeds, the role of photosynthesis in carbon metabolism is not fully understood. Different views exist regarding whether photosynthesis is necessary for fatty acid synthesis in green seeds (Eastmond et al., 1996; Rawsthorne, 2002; Ruuska et al., 2002). Recent evidence shows that the carbon flow through the oxidative pentose phosphate pathway is less than previously assumed (Schwender et al., 2003) and implies that photosynthesis may contribute a significant amount of reducing power under the normal growth condition. Nonetheless, since maternal Suc is not a limiting factor for seed oil production (Roesler et al., 1997; Zou et al., 1997; Jain et al., 2000; Jako et al., 2001), developing embryos may be able to adjust the flux distribution to obtain more reducing power from Suc when photosynthesis is impaired. Even in leaf tissues where photosynthesis provides most of the ATP and reducing power for fatty acid synthesis, exogenous sugar could serve as an alternative resource when photosynthesis is abolished. This is demonstrated by the fact that Arabidopsis albino mutants could grow to fairly normal size in tissue culture in the presence of exogenous sugar (Grevelding et al., 1996; Motohashi et al., 2001). Based on these rationales, we think it is unlikely that the dramatic reduction of oil content in *sse1* is due solely to lack of photosynthesis. Rather, we favor the view that fatty acid deficiency in *sse1* is a direct consequence of peroxisomal defects but may be further exacerbated by insufficient photosynthesis.

CONCLUSIONS

The abnormal peroxisome biogenesis and fatty acid synthesis in *sse1* raises the interesting possibility that peroxisomes are required for both catabolic and anabolic lipid metabolism. This hypothesis is consistent with other observations in both plants and animals and worth further investigation. Because of the complicated metabolic events and organelle interactions during reserve deposition, alternative interpretations of *sse1* phenotypes cannot be excluded. Our study, however, is one step toward further understanding the lipid metabolic roles of peroxisomes and the complicated process of seed oil deposition.

MATERIALS AND METHODS

Plant Materials and Growth Conditions

All seedlings used were grown on petri dishes containing 0.5× Murashige and Skoog salt supplemented with minimum organics (Sigma, St. Louis), 1%

or 2% Suc, and 0.8% agar. When indicated, Tween 80 was added to 0.1%. Embryos were separated from seed coats under a dissecting microscope with two sterile needles. Before dissection, seeds were surface sterilized and soaked in water for several hours or overnight. The *sse1* and wild-type control seedlings in Figure 6 were incubated in dim light (2–4 μE m^{-2} s^{-1}) under a 12-h-light and 12-h-dark cycle. All the other seedlings were grown under continuous light of 35 μE m^{-2} s^{-1} intensity. The developing seeds were obtained from soil-grown plants in a greenhouse where the light cycle varies with the seasons.

For construction of the *sse1adg1* and *sse1pgm1* double mutants, the heterozygous *sse1*/+ plants were used as paternal parents and the starchless mutants (obtained from the Arabidopsis Biological Resource Center, Ohio State University, Columbus, OH) as maternal parents. F_1 seedlings were confirmed by their kanamycin resistance (Lin et al., 1999) and the F_2 plants homozygous for the *adg1* or *pgm1* allele and heterozygous for the *sse1* allele were identified as those individuals that exhibited kanamycin resistance but did not show I_2 staining of starch in rosette leaves (Eimert et al., 1995). The F3 shrunken seeds from these F_2 plants are the desired *sse1adg1* or *sse1pgm1* double mutants.

Plasmid Construction

A fragment of SSE1 cDNA from the second codon to 41 bp downstream of the stop codon was excised from the cDNA clone (Lin et al., 1999) by *Hin*dIII and *Ssp*I digestion and blunt ended with Klenow. This fragment was cloned into the *Eco*RI site (blunt ended) of the pEGAD vector (Cutler et al., 2000), and the SSE1 coding region was placed downstream to and fused in frame with the GFP coding region. This is the GFP-SSE1 construct.

The RFP gene with human-optimized translational codon usage (similar to plant optimization) was excised from the peak12-synrfp-s87 plasmid (E. Park and B. Seed, unpublished data) and cloned between the CaMV 35S promoter and the nopaline synthase 3′ region in a pUC19-based vector. The resulting YL10 plasmid was used to make the two peroxisomal marker constructs. A PTS1 fragment corresponding to the last 10 amino acids from the pumpkin (Cucurbita cv Kurokawa Amakuri) *Malate Synthase* gene (Hayashi et al., 1996) was made by annealing the two synthesized primers PTS1-F (5′-TGTACATCCATCATCCCAGGGAGCTGTCCAGGCTGTGAGCTC-3′) and PTS1-R (5′-CACAGCCTGGACAGCTCCCTGGGATGATGGAT-3′). The *Bsr*GI and *Sac*I sites (underlined) were added at the N and C termini of PTS1-F, respectively. The PTS1 fragment was fused to the C terminus of RFP in YL10 to create the RFP-PTS1 plasmid. For the construction of PTS2-RFP plasmid, the N-terminal 135 bp of the Arabidopsis *KAT2* (GenBank accession AB008854) coding region including the predicted PTS2 was isolated by RT-PCR, using primers KAT2.109 (5′-CAGTCTAGAATCATGGAGAAAGCGATCGAGA-3′) and KAT2.243 (5′-TTGTCCATGGATAGTGGAGTCCTATGTGC-3′). An *Xba*I and a *Nco*I site (underlined) were included in KAT2.109 and KAT2.243, respectively. The PTS2 fragment was ligated with the *Xba*I- and *Nco*I-digested YL10 and fused in frame to the N terminus of RFP. The P35S-RFP-PTS1-NOS3′ or P35S-PTS2-RFP-NOS3′ expression cassettes were excised from corresponding plasmids by *Eco*RI (blunt-ended) and *Hind*III digestion and subsequently cloned into the binary vector pCambia1301 between *Bst*EII (blunt-ended) and *Hind*III sites, resulting in pCAMB-RFPPTS1 and pCAMB-PTS2RFP, respectively.

Microscopy

A Nikon TE200 fluorescence microscope (Tokyo) or a Leica TCSNT confocal microscope (Wetzler, Germany) was used to observe GFP and RFP. For fluorescence microscopy, the fluorescein isothiocyanate filter sets (excitation/emission) for GFP (460–500 nm/510–560 nm), RFP (528–553 nm/600–660 nm), or DAPI stained nuclei (379–401 nm/435–485 nm) were used. For confocal microscopy, a 480 to 500 nm wavelength of excitation and 510 to 550 nm (GFP), 580 to 620 nm (RFP), or 605 to 685 nm (chloroplast) wavelengths of emission were used. Seedlings grown on petri dishes were observed directly under the fluorescence microscope for RFP-labeled peroxisomes in roots. For other observations, plant materials were transferred onto slides, submerged in 50% glycerol, and covered with coverslips. Embryos were dissected from seed coats before observation. For DAPI staining of nuclei, seedlings were submerged in 1 μg mL^{-1} DAPI and 0.2% Triton for 1 h to stain the nuclei.

For electron microscopic observation of peroxisomes, cotyledons or true leaves from young seedlings were cut into 1 to 2 mm squares in 4% paraformaldehyde and 2% glutaraldehyde in 0.1 M cacodylate buffer (pH 7.2). After being prefixed for 2 to 16 h in the same solution and postfixed for 2 h in 1% osmium tetroxide and 0.1 M cacodylate buffer (pH 7.2), samples were dehydrated through an ethanol series and imbedded in Spurr's resin. Thin sections were stained with uranyl acetate and lead citrate before being observed under a transmission electron microscope.

Feeding Developing Seeds with ^{14}C-Labeled Oil Synthesis Precursors

In each feeding experiment, 20 developing seeds (seed coats were not removed) were incubated in 100 μL of feeding buffer for 16 to 18 h under continuous light. The feeding buffers were: 34 mM [U-^{14}C]Glc at 0.32 Ci mol^{-1} in 100 mM HEPES (pH 7.4); 1 mM [2-^{14}C]pyruvate at 0.68 Ci mol^{-1} in 100 mM HEPES (pH 7.4); 1 mM [1-^{14}C]acetate at 1 Ci mol^{-1} in 100 mM HEPES (pH 7.4); and [1-^{14}C]oleic acid at 0.9 Ci mol^{-1} in 100 mM potassium phosphate (pH 7.4). Extraction and thin-layer chromatography separation of triacylglycerol were as described in Focks and Benning (1998). The amount of ^{14}C isotope incorporated into triacylglycerol was determined by scintillation counting. To determine the amount of precursor taken up by the embryos (the proportion remaining in the embryos), embryos were rinsed with water and ground before scintillation counting. To determine the amount of precursor incorporated into starch, cell wall, or protein, embryos were rinsed with water and ground in 0.5 mL 80% ethanol. After 40 min incubation at 70°C and centrifugation, the unincorporated precursor was removed as the soluble fraction. The pellet was rinsed with another 0.5 mL 80% ethanol before measuring the amount of incorporated ^{14}C isotope by scintillation counting.

Quantification of Oil, Starch, or Suc in Seeds or Dissected Embryos

Fatty acid methyl ester (FAME) derivatization and extraction was carried out on 10 to 20 seeds (Fig. 5B) or 10 to 30 dissected embryos (depending on developmental stage; Fig. 5A) that were ground in a 10-μL glass test tube with a glass rod. The ground materials were incubated in a sealed glass vial with 0.7 mL of 1 N methanolic HCl containing 3.5 μg of myristic acid at 85°C for 2 h. Following the addition of 0.7 mL each of hexane and 0.9% NaCl, the FAME was extracted to the hexane phase. The hexane phase was transferred to a 0.5-μL tube and concentrated to about 100 μL under a flow of nitrogen. The FAME was quantified by gas chromatographic-mass spectrometry using a HP5890 Series II gas chromatograph (Agilent Technologies, Burlington, MA) equipped with a Supelcowax SP-10 capillary column (Supelco, Bellefonte, PA) attached to a HP-5971 mass spectrometer (Agilent Technologies). The gas chromatograph oven temperature was programmed to be maintained initially at 150°C for 2 min, then to rise to 200°C at 10°C min^{-1} with a hold at 200°C for 4 min, subsequently to rise to 240°C at 5°C min^{-1} with a hold at 240°C for 3 min, finally to rise to 270°C at 10°C min^{-1} with a hold at 270°C for 5 min. The carrier gas flow rate was maintained at 0.8 mL min^{-1}. The quantity of each fatty acid was determined by comparison with the myristic acid internal control.

For the starch content assay, 10 to 20 seeds (Fig. 5B) or 15 to 40 dissected embryos (depending on developmental stage; Fig. 5A) were homogenized in 150 μL of 80% ethanol and incubated at 70°C for 2 h to dissolve the soluble sugars. After centrifugation, the starch-containing pellet was rinsed twice with 150 μL of 80% ethanol. The pellet was vacuum dried and starch was solublized in 50 μL of 0.2 N KOH for 1 h at 95°C. After addition of 5 μL of 2 N acetic acid and centrifugation, 35 μL of supernatant was combined with 15 μL of water and 50 μL of starch assay reagent (Sigma) and incubated at 60°C for 15 min. The reaction mixture was transferred to a 1-cm light path cuvette and mixed with 0.5 mL of Glc assay buffer containing 50 mM Tris (pH 7.8), 1.5 mM NAD, and 1 mM ATP. The background A_{340} was determined after 3 to 5 min. After further incubation with 1.25 units of hexokinase and 0.67 units of Glc 6-phosphate dehydrogenase for 10 to 15 min, the production of NADH was measured spectrophotometrically at 340 nm.

For quantification of Suc, soluble sugar was extracted from 50 seeds and vacuum dried. Suc was quantified using a Suc assay kit from Sigma.

RT-PCR Analysis of Gene Expression

Embryos of different developmental stages were separated from siliques and RNA was isolated according to Parcy et al. (1994) and Downing et al. (1992) except that RNA was precipitated with 2 M LiCl on ice for 1 h. One

microgram of the DNase treated RNA was used in a 20-μL RT reaction at 42°C using Superscript RTII (Invitrogen, Carlsbad, CA) as the RT and oligo(dT)$_{18}$ as the primer. Subsequently, 0.5 μL of the same RT mixture was used in each 20-μL PCR reaction to amplify different cDNA fragments. The PCR reactions were carried out for 30 to 40 cycles and 8 μL of each product was checked in a 1% agarose gel. The primers FP7 and FP14R were used to amplify *SSE1* (*AtPEX16*) cDNA (Lin et al., 1999). The primers used for the other peroxin genes were: PEX1-5′: 5′-GACGTGATGGAAACAGAAG-3′; PEX1-3′: 5′-TTGACGAGGCTCTTTCTTG-3′; PEX3-5′: 5′-CTTGCTGATTTGGAACGAG-3′; PEX3-3′: 5′-CATCCGTGAAGCACTTGAG-3′; PEX5-5′: 5′-GATGAGAGACCTTGTTAACG-3′; PEX5-3′: 5′-TCACACCATGTTGTTGCTC-3′; PEX7-5′: 5′-TCAGTCCATTCTACGAGTC-3′; PEX7-3′: 5′-CTCTGTATGATGATCATACC-3′; PEX10-5′: 5′-CAACAATGGTGAATAAAGCTC-3′; PEX10-3′: 5′-TGTGATCATAGCCTTTTGAAG-3′; PEX12-5′: 5′-AGAAGATGTTGTTTCAGGTG-3′; PEX12-3′: 5′-ATTGATACCACCATTCCATC-3′; PEX19-5′: 5′-GAACAGTCACACCGATGAC-3′; and PEX19-3′: 5′-CACATGATACAGCAATTTGG-3′. The primers for *LEC1* gene are: LEC1-5′: 5′-CAACAACCCAACCCCAATG-3′; LEC1-3′: 5′-CCATCTTCACTTATACTGAC-3′. The primers for *ACT2* gene are: ACT2-5′: 5′-AAGAGATAATCCAGGAGATTC-3′; ACT2-3′: 5′-CAAGGAGAGAACAGCTTGG-3′.

Sequence data from the this article have been deposited with the GenBank data libraries under accession numbers AB008854 (*KAT2*), U41998 (*ACT2*), and AC013484 (*LEC1*), and as indicated in Mullen et al. (2001a) for *PEX* genes.

ACKNOWLEDGMENTS

We thank the Arabidopsis Biological Resource Center (Columbus, OH) for the pEGAD vector; Drs. Eun-Chung Park and Brian Seed (Massachusetts General Hospital, Boston) for providing the unpublished codon optimized RFP; and Drs. Julie Nardone, Hans J. Bohnert, and Lance Davidow for critical reading of the manuscript.

Received November 26, 2003; returned for revision February 24, 2004; accepted February 24, 2004.

LITERATURE CITED

An YQ, McDowell JM, Huang S, Mckinney EC, Chambliss S, Meagher RB (1996) Strong, constitutive expression of the Arabidopis ACT2/ACT8 actin subclass in vegetative tissues. Plant J **10:** 107–121

Arai Y, Nakashita H, Suzuki Y, Kobayashi Y, Shimizu T, Yasuda M, Doi Y, Yamaguchi I (2002) Synthesis of a novel class of polyhydroxyalkanoates in peroxisomes, and their use in monitoring short-chain-length intermediates of β-oxidation. Plant Cell Physiol **43:** 555–562

Ashrafi K, Chang FY, Watts JL, Fraser AG, Kamath RS, Ahringer J, Ruvkun G (2003) Genome-wide RNAi analysis of *Caenorhabditis elegans* fat regulatory genes. Nature **421:** 268–272

Buchanan BB, Gruissem W, Jones RL (2000) Biochemistry and Molecular Biology of Plants. American Society of Plant Physiologists, Rockville, Maryland

Caspar T, Huber SC, Somerville C (1985) Alterations in growth, photosynthesis, and respiration in a starchless mutant of *Arabidopsis thaliana* (L.) deficient in chloroplast phosphoglucomutase activity. Plant Physiol **79:** 11–17

Chiu W, Niwa Y, Zeng W, Hirano T, Kobayashi H, Sheen J (1996) Engineered GFP as a vital reporter in plants. Curr Biol **6:** 325–330

Cutler SR, Ehrhardt DW, Griffitts JS, Somerville CR (2000) Random GFP::cDNA fusions enable visualization of subcellular structures in cells of *Arabidopsis* at a high frequency. Proc Natl Acad Sci USA **97:** 3718–3723

Downing WE, Mauxion F, Fauvarque M-O, Reviron M-P, de Vienne D, Vartanian N, Giraudat J (1992) A *Brassica napus* transcript encoding a protein related to the Kunitz protease inhibitor family accumulates upon water stress in leaves, not seeds. Plant J **2:** 685–693

Eastmond PJ, Graham IA (2001) Re-examining the role of glyoxylate cycle in oilseeds. Trends Plant Sci **6:** 72–77

Eastmond PJ, Kolacna L, Rawsthorne S (1996) Photosynthesis by developing embryos of oilseed rape (*Brassica napus L.*). J Exp Bot **47:** 1763–1769

Eccleston VS, Ohlrogge JB (1998) Expression of lauryol-acyl carrier protein thioesterase in *Brassica napus* seeds induces pathways for both fatty acid oxidation and biosynthesis and implies a set point for triacylglycerol accumulation. Plant Cell **10:** 613–621

Eimert K, Wang S-M, Lue W-L, Chen J (1995) Monogenic recessive mutations causing both late floral initiation and excess starch accumulation in Arabidopsis. Plant Cell **7:** 1703–1712

Eitzen GA, Szilard RK, Rachubinski RA (1997) Enlarged peroxisomes are present in oleic acid-grown Yarrowia lipolytica overexpressing the PEX16 gene encoding an intraperoxisomal peripheral membrane peroxin. J Cell Biol **137:** 1265–1278

Focks N, Benning C (1998) *wrinkled1*: a novel, low-seed-oil mutant of Arabidopsis with a deficiency in the seed-specific regulation of carbohydrate metabolism. Plant Physiol **118:** 91–101

Gerhardt B (1992) Fatty acid degradation in plants. Prog Lipid Res **31:** 417–446

Germain V, Rylott EL, Larson TR, Sherson SM, Bechtold N, Carde J-P, Bryce JH, Graham IA, Smith SM (2001) Requirement for 3-ketoacyl-CoA thiolase-2 in peroxisome development, fatty acid beta-oxidation and breakdown of triacylglycerol in lipid bodies of Arabidopsis seedlings. Plant J **28:** 1–12

Grevelding C, Suter-Crazzolara C, von Menges C, Kemper E, Masterson R, Schell J, Reiss B (1996) Characterization of a new allele of *pale cress* and its role in greening in *Arabidopsis thaliana.* Mol Gen Genet **251:** 532–541

Guo T, Kit YY, Nicaud JM, Le Dall MT, Sears SK, Vali H, Chan H, Rachubinski RA, Titorenko VI (2003) Peroxisome division in the yeast *Yarrowia lipolytica* is regulated by a signal from inside the peroxisome. J Cell Biol **162:** 1255–1266

Hayashi M, Masahiro A, Kato A, Kondo M, Nishimura M (1996) Transport of chimeric proteins that contains a carboxy-terminal targeting signal into plant microbodies. Plant J **10:** 225–234

Hayashi M, Nito K, Takei-Hoshi R, Yagi M, Kondo M, Suenaga A, Yamaya T, Nishimura M (2002) Ped3p is a peroxisomal ATP-binding cassette transporter that might supply substrates for fatty acid β-oxidation. Plant Cell Physiol **43:** 1–11

Hayashi M, Toriyama K, Kondo M, Nishimura M (1998) 2,4-Dichlorophenoxybutyric acid-resistant mutants of Arabidopsis have defects in glyoxysomal fatty acid b-oxidation. Plant Cell **10:** 183–195

Honsho M, Tamura S, Shimozawa N, Suzuki Y, Kondo N, Fujiki Y (1998) Mutation in PEX16 is causal in the peroxisome-deficient Zellweger syndrome of complementation group D. Am J Hum Genet **63:** 1622–1630

Hu J, Aguirre M, Peto C, Alonso J, Ecker J, Chory J (2002) A role for peroxisomes in photomorphogenesis and development of Arabidopsis. Science **297:** 405–409

Jain RK, Coffey M, Lai K, Kumar A, MacKenzie SL (2000) Enhancement of seed oil content by expression of glycerol-3-phosphate acyltransferase genes. Biochem Soc Trans **28:** 958–961

Jako C, Kumar A, Wei Y, Zou J, Barton DL, Giblin EM, Covello PS, Taylor DC (2001) Seed-specific over-expression of an Arabidopsis cDNA encoding a diacylglycerol acyltransferase enhances seed oil content and seed weight. Plant Physiol **126:** 861–874

Kamada T, Nito K, Hayashi H, Mano S, Hayashi M, Nishimura M (2003) Functional differentiation of peroxisomes revealed by expression profiles of peroxisomal genes in *Arabidopsis thaliana.* Plant Cell Physiol **44:** 1275–1289

Karnik SK (2003) Two distinct (non-overlapping) targeting signals sort AtPex16p to peroxisomes indirectly via a preperoxisomal compartment. *In* Plant Biology 2003, July 25–30, 2003, Honolulu, HI. American Society of Plant Biologists, Rockville, MD

Ke J, Behal RH, Back SL, Nikolau BJ, Wurtele ES, Oliver DJ (2000) The role of pyruvate dehydrogenase and acetyl-coenzyme A synthetase in fatty acid synthesis in developing Arabidopsis seeds. Plant Physiol **123:** 497–508

Kennedy EP (1961) Biosynthesis of complex lipids. Fed Proc Am Soc Exp Biol **20:** 934–940

Kovacs WJ, Olivier LM, Krisans SK (2002) Central role of peroxisomes in isoprenoid biosynthesis. Prog Lipid Res **41:** 369–391

Lin TP, Caspar T, Somerville J, Preiss J (1988) Isolation and characterization of a starchless mutant of *Arabidopsis thaliana* (L) Heynh lacking ADPglucose pyrophosphorylase activity. Plant Physiol **86:** 1131–1135

Lin Y, Sun L, Nguyen LV, Rachubinski RA, Goodman HM (1999) The pex16p homolog SSE1 and storage organelle formation in Arabidopsis seeds. Science **284:** 328–330

Lisenbee CS, Karnik SK, Trelease RN (2003) Overexpression and mislocalization of a tail-anchored GFP redefines the identity of peroxisomal ER. Traffic **4:** 491–501

Lotan T, Ohto M, Yee KM, West MA, Lo R, Kwong RW, Yamagishi K, Fischer RL, Goldberg RB, Harada JJ (1998) Arabidopsis LEAFY COTYLEDON 1 is sufficient to induce embryo development in vegetative cells. Cell **93:** 1195–1205

Mansfield SG, Briarty LG (1992) Cotyledon cell development in *Arabidopsis thaliana* during reserve deposition. Can J Bot **70:** 151–164

Motohashi R, Nagata N, Ito T, Takahashi S, Hobo T, Toshida S, Shinozaki K (2001) An essential role of a TatC homologue of a ΔpH-dependent protein transporter in thylakoid membrane formation during chloroplast development in *Arabidopsis thaliana.* Proc Natl Acad Sci USA **98:** 10499–10504

Mullen RT, Flynn CR, Trelease RN (2001a) How are peroxisomes formed? The role of the endoplasmic reticulum and the peroxins. Trends Plant Sci **6:** 256–261

Mullen RT, Lisenbee CS, Flynn CR, Trelease RN (2001b) Stable and transient expression of chimeric peroxisomal membrane proteins induces an independent ''zippering'' of peroxisomes and an endoplasmic reticulum subdomain. Planta **213:** 849–863

Ohlrogge JB, Jaworski JG (1997) Regulation of fatty acid synthesis. Annu Rev Plant Physiol Plant Mol Biol **48:** 109–136

Olsen LJ (1998) The surprising complexity of peroxisome biogenesis. Plant Mol Biol **38:** 163–189

Parcy F, Valon C, Raynal M, Gaubier-Comella P, Delseny M, Giraudat J (1994) Regulation of gene expression programs during Arabidopsis seed development: roles of the ABI3 locus and of endogenous abscisic acid. Plant Cell **6:** 1567–1582

Periappuram C, Steinhauer L, Barton DL, Taylor DC, Chatson B, Zou J (2000) The plastidic phosphoglucomutase from Arabidopsis. A reversible enzyme reaction with an important role in metabolic control. Plant Physiol **122:** 1193–1199

Poirier Y, Ventre G, Caldelari D (1999) Increased flow of fatty acids toward β-oxidation in developing seeds of Arabidopsis deficient in diacylglycerol acyltransferase activity or synthesizing medium-chain-length fatty acids. Plant Physiol **121:** 1359–1366

Rawsthorne S (2002) Carbon flux and fatty acid synthesis in plants. Prog Lipid Res **41:** 182–196

Richmond TA, Bleecker AB (1999) A defect in β-oxidation causes abnormal inflorescence development in Arabidopsis. Plant Cell **11:** 1911–1923

Roesler K, Shintani D, Savage L, Boddupalli S, Ohlrogge J (1997) Targeting of the Arabidopsis homomeric acetyl-CoA carboxylase to plastids of rapeseeds. Plant Physiol **113:** 75–81

Ruuska SA, Girke T, Benning C, Ohlrogge JB (2002) Contrapuntal networks of gene expression during Arabidopsis seed filling. Plant Cell **14:** 1191–1206

Rylott EL, Rogers CA, Gilday AD, Edgell T, Larson TR, Graham IA (2003) Arabidopsis mutants in short- and medium-chain acyl-CoA oxidase activities accumulate acyl-CoAs and reveal that fatty acid beta-oxidation is essential for embryo development. J Biol Chem **278:** 21370–21377

Schwender J, Ohlrogge JB, Shachar-Hill Y (2003) A flux model of glycolysis and the oxidative pentosephosphate pathway in developing Brassica napus embryos. J Biol Chem **278:** 29442–29453

South ST, Gould SJ (1999) Peroxisome synthesis in the absence of preexisting peroxisomes. J Cell Biol **144:** 255–266

Sparkes IA, Brandizzi F, Slocombe SP, El-Shami M, Hawes C, Baker A (2003) An Arabidopsis pex10 null mutant is embryo lethal, implicating peroxisomes in essential role during plant embryogenesis. Plant Physiol **133:** 1809–1819

Terzaghi WB (1989) Manipulating membrane fatty acid compositions in whole plants with tween-fatty acid esters. Plant Physiol **82:** 780–786

Titorenko VI, Ogrydziak DM, Rachubinski RA (1997) Four distinct secretory pathways serve protein secretion, cell surface growth, and peroxisome biogenesis in the yeast *Yarrowia lipolytica.* Mol Cell Biol **17:** 5210–5226

Titorenko VI, Chan H, Rachubinski RA (2000) Fusion of small peroxisomal vesicles in vitro reconstructs an early step in the in vivo multistep peroxisome assembly of Yarrowia lipolytica. J Cell Biol **148:** 29–43

Wanders RJA (1999) Peroxisomal disorders: clinical, biochemical, and molecular aspects. Neurochem Res **24:** 565–580

Wang SM, Liu WL, Yu TS, Long JH, Wang CN, Eimert K, Chen J (1998) Characterization of ADG1, an Arabidopsis locus encoding for ADPG pyrophosphorylase small subunit, demonstrates that the presence of the small subunit is required for large subunit stability. Plant J **13:** 63–70

Weber H (2002) Fatty acid-derived signals in plants. Trends Plant Sci **7:** 217–224

Zou J, Katavic V, Giblin EM, Barton DL, Mackenzie SL, Keller WA, Hu X, Taylor D (1997) Modification of seed oil content and acyl composition in the Brassicacea by expression of a yeast sn-2 acyltransferase gene. Plant Cell **9:** 909–923